Synthesis of carrageenan/multi-walled carbon nanotube hybrid hydrogel nanocomposite for adsorption of crystal violet from aqueous solution

Hossein Hosseinzadeh

Payame Noor University, Chemistry Department, 19395-4697, Tehran, Iran
e-mail: h_hoseinzadeh@pnu.ac.ir

A novel polysaccharide-based hydrogel nanocomposite was prepared using grafting of acrylic acid (AA) on to kappa-carrageenan (κC) by incorporating multi-walled carbon nanotube (MCNT). In fact, MCNTs were used as nano-sized reinforcements in the synthesized nanocomposite. Spectroscopy together with morphology proved relatively strong κC-MCNT interaction. Besides, the swelling behavior of the nanocomposite hydrogel was studied. The results showed that in the presence of MCNTs, the equilibrium swelling capacity was decreased. This can be attributed to cross-linking role and hydrophilicity nature of MCNTs. The adsorption performance of hydrogel nanocomposite was also investigated for the removal of crystal violet (CV) as a cationic dye. The effects of some important parameters such as MCNT concentration, pH and contact time on the uptake of CV solution were studied. Equilibrium adsorption isotherm data of the hydrogel exhibited better fit to the Langmuir than to the Freundlich isotherm model. According to this model, the maximum adsorption capacity of κC-based hydrogel nanocomposite was found to be 118 mg · g^{-1}.

Keywords: carrageenan, hydrogel, nanocomposite, carbon nanotube, adsorption, crystal violet.

INTRODUCTION

Hydrogels are three-dimensional polymeric networks capable of imbibing large quantities of water in its structure[1]. Polymer hydrogels have gained tremendous importance in wide variety of biomedical applications such as wound dressings[2], contact lenses[3], artificial organs[4], tissue engineering[5] and drug delivery systems[6–8] due to their unique water absorption and retention capacity.

However, poor mechanical properties of hydrogels are serious impediments that must be resolved for their commercial applications[9]. To date, cross-linking techniques have been used to increase mechanical strength of hydrogels, but these techniques result in only a moderate enhancement and sometimes even a lowered adsorption capacity[9]. Recently, carbon nanotubes (CNTs) have received special interest as one of the most promising nano-fillers into polymer matrices for enhancement of its mechanical property[10–12]. In fact, as a result of the early report concerning the preparation of a CNTs/polymer composite by Ajayan et al.[13], many efforts have been made to combine CNTs and polymers to produce functional composite materials with superior properties[14, 15].

Polymer-based nanocomposite is commonly defined as the combination of a polymer matrix and additives that have at least one dimension in the nanometer range. In order to exploit excellent mechanical properties of CNTs, varieties of polymer matrices were used to provide with reinforcements as reported in a review[16].

Since their discovery, CNTs have emerged as a promising molecule in the development of innovative functional nano-devices[17]. Depending on the synthesis process, CNTs are composed of either a single shell (single-walled carbon nanotube) or several rolled sheets (multi-walled carbon nanotube). Multi-walled carbon nanotubes, in particular, have received considerable attention due to their electrical, mechanical, and optical properties[18–22]. Moreover, CNTs are effective in adsorbing different materials[23–25].

Here, we demonstrate the preparation of a carrageenan-based hydrogel impregnated with CNTs and analyze their swelling behavior and adsorption performance of crystal violet (CV) as a model dye. There are many processes to remove CV molecules from colored solutions[26–30]. However, low adsorption capacities of these adsorbents toward dyes limit their applications in practical fields.

EXPERIMENTAL

Material

The polysaccharide, kappa-carrageenan (κC, from Condinson Co., Denmark), N,N'-methylene bisacrylamide (MBA, from Merck), and ammonium persulfate (APS, from Fluka) were of analytical grade and used without further purification. Acrylic acid (AA, from Merck), was used after vacuum distillation. Multi-walled carbon nanotube (MCNT, outer diameter 10–20 nm, length 10–30 m, purity >95 wt% and ash <1.5 wt%) was a gift sample from Atoor Sanat Inc., Iran.
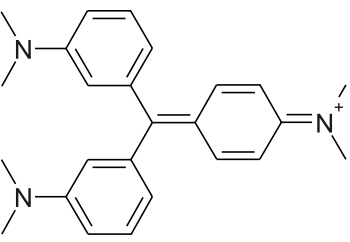
Dyestuffs

Crystal violet (CV, from Sigma-Aldrich Chemical Company, USA) was used without further purification. The molecular structure and identification information of CV are depicted in Table 1.

Preparation of Hydrogel

A general procedure for the synthesis of the κC-based hydrogel nanocomposites was conducted as follows. Firstly, 0.10 g of MCNT were dispersed in 25 mL of double-distilled water using 750 Watt ultrasonic processor (VC 750, Sonics) with a high power sonic tip operated at 20 kHz frequency and 30% amplitude for 30 min. The resulted dispersion of the MCNT was added to a κC solution to get a stable dispersion. Then, 0.10 g of APS as an initiator was added to the solution and allowed to stir for 10 min. After adding of APS, certain amount of AA (3 mL) was added simultaneously to the carrageenan solution. MBA solution (0.05 g in 5 mL H$_2$O) was then added to the reaction mixture. After 60 min, the reaction product was allowed to cool to ambient temperature

Table 1. The chemical structure and some properties of CV

IUPAC name	Chemical structure	Molar mass [g/mol]	Color Index Number	λ_{max} [nm]
Tris(4-(dimethylamino) phenyl)methylium		407.98	42555	590

and neutralized to pH 8 by addition of NaOH solution (1 N). At the end of the reaction, the gel product was poured into ethanol (300 mL) and was dewatered for 12 h. Then, the product was cut into small pieces, washed with 200 mL of ethanol and filtered off. The particles were dried in an oven at 50°C for 12 h. After grinding, the powdered hydrogel nanocomposite was stored in absence of moisture, heat and light.

Adsorption studies

Adsorption experiments were conducted by adding of 0.2 g hydrogel nanocomposite into 0.01 L of the CV solution at 30°C. All of the adsorption experiments were conducted in triplicate and performed for 24 h in shaking conditions (200 rpm). To study the adsorption kinetics, at specified time intervals, the amount of residual dye in the solution was determined after 24 h at $\lambda_{max}=590$ nm. The dye concentration determinations were performed using a Perkin Elmer Lambda 35 UV/VIS spectrophotometer.

The amount of adsorbed CV was calculated based on a mass balance equation as given below:

$$q_e = \frac{(C_0 - C_{eq}) \times V}{W} \quad (1)$$

where q_e is the equilibrium adsorption capacity (mg · g^{-1}), C_0 is the initial concentration of CV in the solution (mg · L^{-1}), C_{eq} is the equilibrium concentration of CV in the solution (mg · L^{-1}), V is the volume of the solution (L), and W is the dry weight of the hydrogel nanocomposite (g).

The non-linear forms of the Langmuir and Freundlich isotherm models were also used to analyze the equilibrium adsorption isotherm data which are represented by the following equations, respectively[31]:

$$q_e = \frac{q_m K_L C_e}{1 + K_L C_e} \quad (2)$$

$$q_e = K_F C_c^{1/n} \quad (3)$$

where q_e is the equilibrium CV concentration (mg · L^{-1}) on the adsorbent, C_e is the equilibrium concentration of CV (mg · L^{-1}) in the solution. q_m (mg · L^{-1}) and K_L (L · g^{-1}) are Langmuir isotherm coefficients. The value of q_m represents the maximum adsorption capacity of the adsorbent. K_F [(mg · g^{-1})/(mg · L^{-1})$^{1/n}$] and n are Freundlich isotherm coefficients. K_F is related to the adsorption capacity of the adsorbent and n is an empirical parameter representing the heterogeneity of site energies. The fits of experimental data to the above mentioned isotherm models were evaluated by the non-linear coefficients of determination (R^2).

Instrumental Analysis

Fourier transform infrared (*FTIR*) spectra of samples were taken in KBr pellets, using an ABB Bomem MB-100 FTIR spectrophotometer (Quebec, Canada) at room temperature with an average of 64 scans at 4 cm^{-1} resolution. The surface morphology of the gel was examined using scanning electron microscopy (SEM). Dried superabsorbent powder were coated with a thin layer of palladium gold alloy and imaged in a SEM instrument (Leo, 1455 VP). Thermogravimetric analysis (TGA) was performed on a Universal V4.1D TA Instruments (SDT Q600) with 8–10 mg samples on a platinum pan under nitrogen atmosphere. Experiments were performed at a heating rate of 10°C/min until 600°C.

RESULTS AND DISCUSSION

Mechanism of hydrogel nanocomposite synthesis

Scheme 1 shows a simple structural proposal of the graft copolymerization of AA on the κC backbones in the presence of MCNT and cross-linking of the graft copolymer. In the first step, the thermally dissociating initiator, i.e. APS, is decomposed under heating (80°C) to produce sulfate anion-radicals. Then, the produced anion-radicals abstract hydrogen from the κC backbones to form corresponding macro-initiators. These macro-radicals initiate grafting of AA onto κC backbones leading to a graft copolymer. Cross-linking reaction also occurred in the presence of MBA. During graft polymerization, MCNTs consumed initiator-derived radicals, which were added to π-bounds of MCNT network.
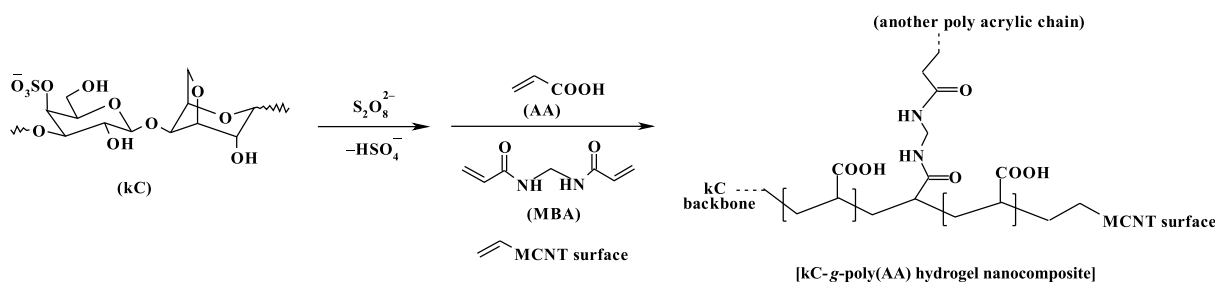
Characterization

FTIR analysis

For identification of the hydrogel nanocomposite, infrared spectroscopy was used. Figure 1 shows the FTIR
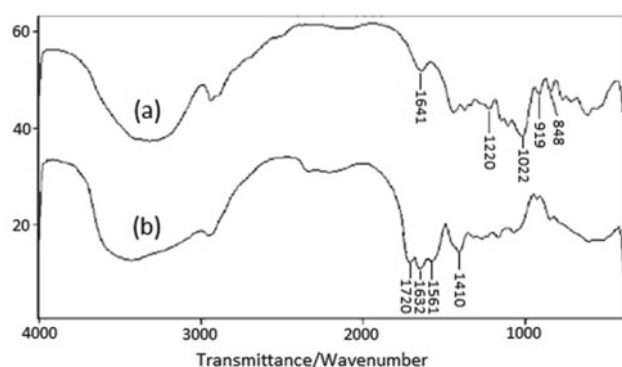
Figure 1. FTIR spectra of κC (a) and κC-g-poly(AA) hydrogel nanocomposite (b)

Scheme 1. Proposed mechanistic pathway for the synthesis of κC-*g*-poly(AA) hydrogel nanocomposite

spectra of non-modified κC and κC-*g*-poly(AA) hydrogel nanocomposite. The bands observed at 848, 919, 1022 and 1220 cm^{-1} can be attributed to D-galactose-4-sulfate, 3,6-anhydro-D-galactose, glycosidic linkage and ester sulfate stretching of κC, respectively (Fig. 1a). The broad band at 3200–3400 cm^{-1} is due to stretching of –OH groups of substrate. The hydrogel nanocomposite product comprises a κC backbone with side chains that carry carboxylic and carboxylate functional groups that are evidenced by peaks at 1720, 1561 and 1410 cm^{-1}, respectively (Fig. 1b). The very intense characteristic band at 1561 cm^{-1} is due to C=O asymmetric stretching in carboxylate anion that is reconfirmed by another sharp peak at 1410 cm^{-1}. This peak is related to the symmetric stretching mode of the carboxylate anion. The observed peak at 1632 cm^{-1} also represents C=C stretches of unsaturated grapheme structure of MCNT.

Scanning electron microscopy analysis

The scanning electron microscopy (SEM) was used to know the morphology and CNT distribution in the hydrogels. Figure 2 shows SEM images of fracture surface of κC, the free-MCNT hydrogel and MCNT-impregnated hydrogel nanocomposites. As seen, SEM of κC–MCNT hydrogel nanocomposite demonstrated a relatively well-developed network with the coil MCNT uniformly distributed in the gel matrix with some small aggregates of CNTs. The SEM pattern of hydrogel nanocomposite also showed that there is only a little microphase disassociation between κC and MCNT. It should be pointed out that the SEM images of both κC-based hydrogel and nanocomposite showed the heterogeneous and porous structure.

Thermogravimetric analysis

The structure of hydrogel nanocomposite was also supported by thermogravimetric analysis (TGA) (Fig. 3). Compared to intact κC and the pure hydrogel, the hydrogel nanocomposite had high initial decomposition temperature and lower weight loss. It is assumed that the addition of CNTs in the hydrogel nanocomposites might lead to increase in the thermal stability. The percent residual mass of the hydrogel was higher than that observed for the pure hydrogel. In fact, TGA curves of
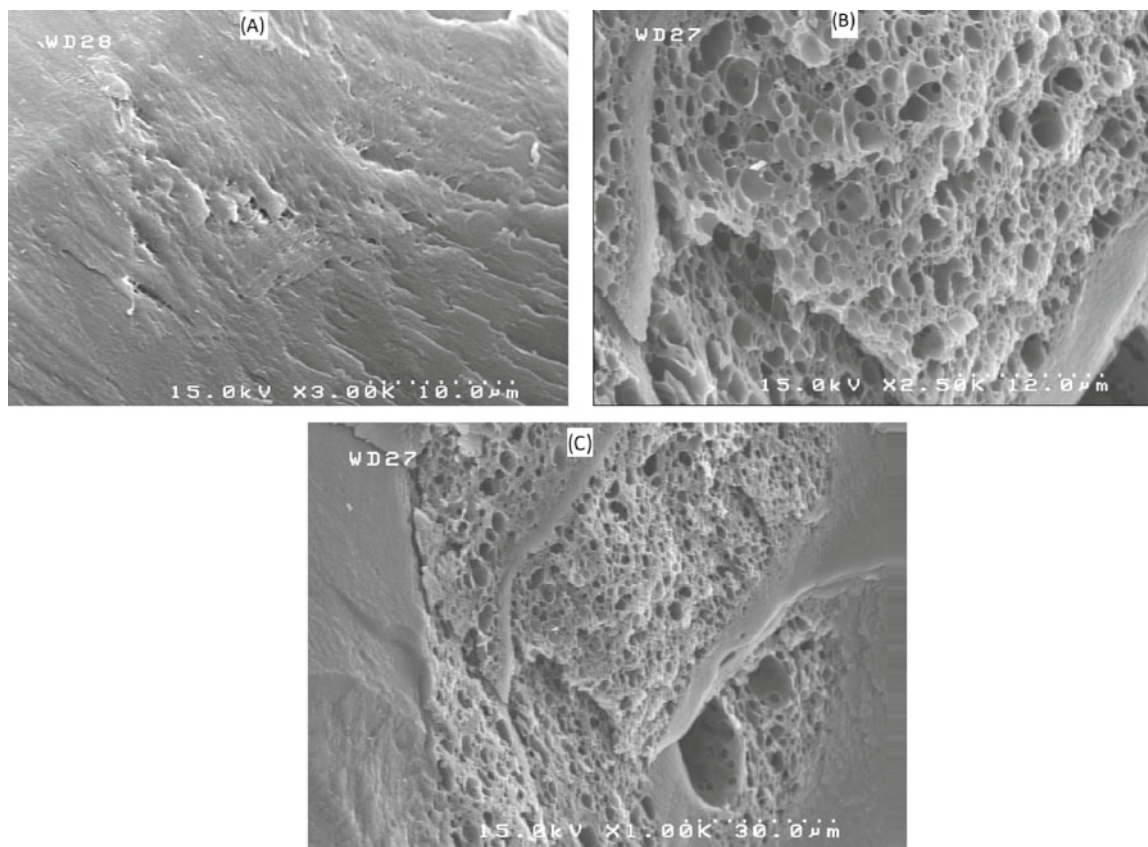
Figure 2. SEM images of the fracture surface of ϰC (A), the free MCNT ϰC-based hydrogel (B), and the hydrogel nanocomposite containing 0.04 wt.% content of MCNT (C)
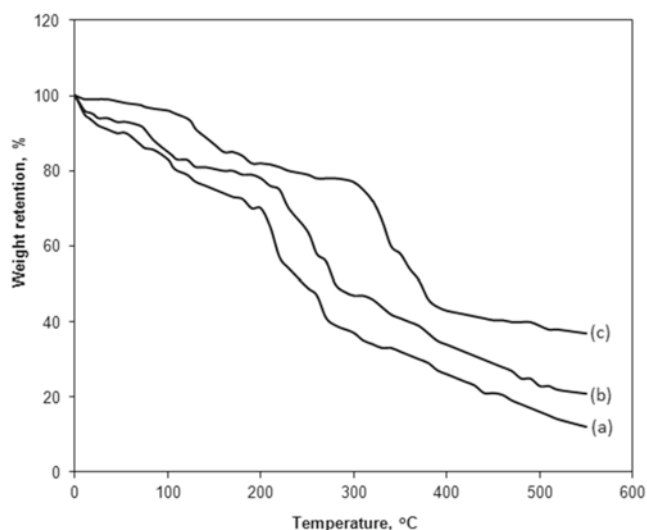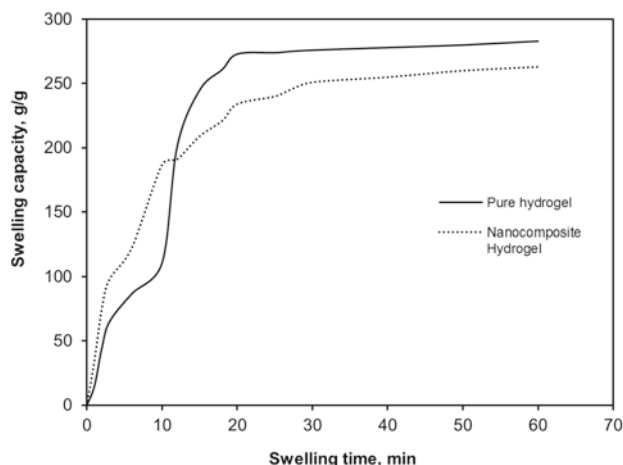
Figure 3. TGA curves of κC (a), pure hydrogel (b), and hydrogel nanocomposite (c)

the nanocomposite samples exhibited only small weight losses (about 5%) at temperatures between 20 and 120°C due to the vaporization of the residual water. Both of the hydrogel samples showed similar weight losses trends at temperatures ranging from 250 to 500°C. This behavior is due to the thermal decomposition of the samples involves depolymerization and decomposition of the units of κC at 250–350°C, which is followed by the oxidative decomposition of the residues at temperatures between 350 and 500°C[32, 33]. However, there was a difference in the weight loss between the pure hydrogel (79%) and the hydrogel nanocomposite (63%) at 550°C, indicating that impregnation of the hydrogels with MCNTs increased the thermal stability.

Swelling study

In general, the swelling capacity of the hydrogel nanocomposite is strongly influenced by their chemical composition. Hence, to understand the influence of the CNTs on the swelling behavior of the hydrogels, the swelling capacity of some specimens was investigated. The swelling behavior of κC-based hydrogel and the hydrogel nanocomposite counterpart can be seen from Figure 4. It is clearly observed that both hydrogels has the same general swelling trend. Comparing with the

degree of swelling of hydrogels, it was found that the ultimate swelling capacity is decreased as the MCNTs are introduced into carrageenan backbones. This decrement in water absorbency can be attributed to the decrease in the ratio of hydrophilic and anionic polymer components[16]. Also, it is assumed that the interaction between MCNT nano-filers and polymeric chains can be occurred (see Scheme 1) and this interaction can lead to increase in cross-linking points and resulting in decreased swelling capacity[16, 34, 35]. When the cross-linkage between the polymeric chains is increased, the swelling capability of the hydrogels will be reduced. Additionally, as SEM shows, MCNTs were distributed irregularly in the gel matrix and formed a well-developed three-dimensional network. As a result, MCNTs can prevent solvent diffusing into gel matrix, and then MCNTs inhibit the dissolution of κC in the matrix. This effect of MCNTs can be called as shielding effect.

Within the first 10 min, however, the swelling ratio of hydrogel nanocomposite is higher than that of native κC hydrogel. This is due to the capillarity of MCNTs in the matrix, which is help for the solvent diffusing into the gel matrix. After 10 min, as mentioned the swelling ratio of nanocomposite is lower than that of pure κC gel. This indicated that MCNTs inhibited the swelling of hydrogel matrix. In summary, within the first 10 min the capillarity effect and after 10 min, the shielding effect is the leading effect, respectively.

Dye adsorption study

Effect of MCNT concentration on the adsorption

The effect of MCNT concentration incorporated in the hydrogel nanocomposite on the absorption of CV concentration was investigated (Fig. 5). As shown, the adsorption capacity of the nanocomposites increased with increase in MCNT concentration up to 0.04 wt.% and thereafter the adsorption capacity decreased. The initial increase in adsorption could be originated from the hydrophobic interactions between the hydrophobic hexagonal arrays of carbon atoms in the MCNTs and the hydrophobic moieties benzene rings of CV. This can be verified by the comparison of the adsorption capacity of the pure hydrogels (MCNT = 0 wt.%) and the nanocomposites containing MCNTs. In fact, MCNTs are already reported as good adsorbents for various materials due

Figure 4. The swelling behavior of κC-based hydrogel and hydrogel nanocomposite
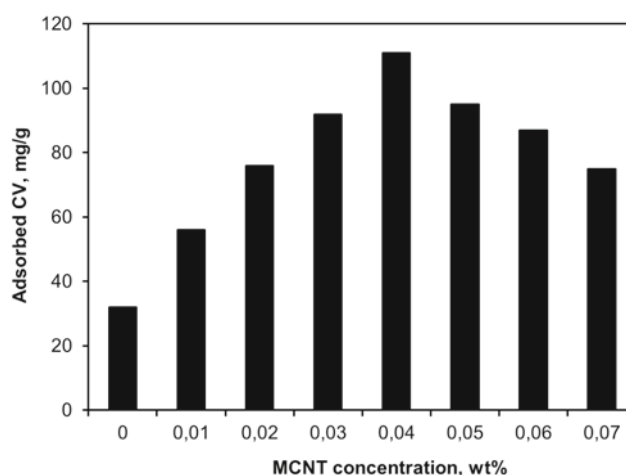
Figure 5. Effect of MCNT concentration on CV adsorption

to its large specific surface area, and hollow and layered nano-sized structures[23, 24, 36, 37]. Therefore, the adsorption capacity of the hydrogel nanocomposite was shown to be higher than that of the puer hydrogels without any MCNTs. A further increase of MCNT concentration, however, results in decreased adsorption capacity. It is probably due to the formation of larger aggregates of MCNTs, which obstruct the access of the CV to the adsorption sites of the nanocomposites.

Effect of agitation time on the adsorption

Figure 6 demonstrates the effect of the contact time on CV adsorption capacity of the hydrogel nanocomposites. The adsorption capacity is intensely increased versus agitation time up to 90 min and then, further increase in the agitation time has practically no remarkable effect on the q_e. It is obvious that increasing the reaction time provides better opportunity for interaction between the adsorbent and the adsorbate. Moreover, aggregation of dye molecules with the increase in contact time makes it almost impossible to diffuse deeper into the adsorbent structure.
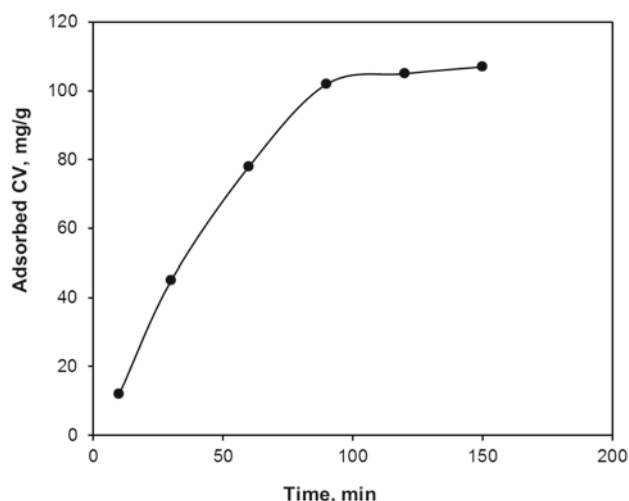

Figure 6. Effect of contact time on CV adsorption

Effect of pH on the adsorption

The pH of the dye solution plays important role in the whole adsorption process and particularly on the adsorption capacity[38]. By changing of the initial pH of dye solution, the nature of active center on the adsorbent can be changed and finally affect the adsorption behavior of adsorbate[39]. Therefore, the effect of pH of initial dye solution on the adsorption capacity was studied by varying the pH from 2 to 13 (Fig. 7). During adsorption, existence of anionic sulfate and carboxylate groups is necessary for interaction of the hydrogel nanocomposite with positively charged CV molecules. Thus in acidic media, the most of these anionic groups are protonated, so lead to a decreased adsorption capacity.
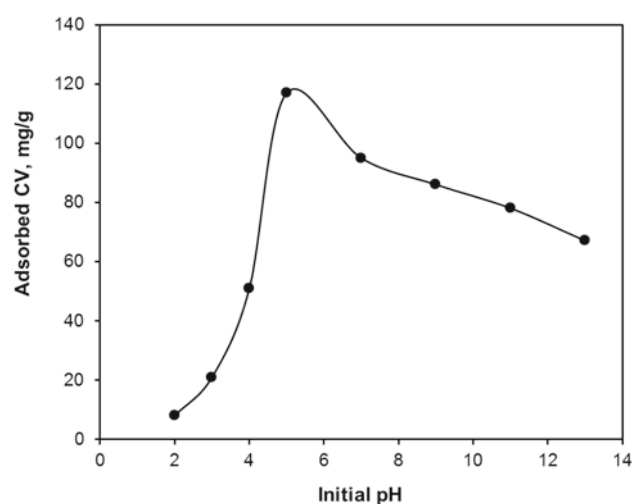

Figure 7. Effect of initial pH of CV solution on adsorption capacity of hydrogel nanocomposites

In fact, lower adsorption of CV at acidic pHs is due to the presence of excess H^+ ions competing with the cation groups on the dye for adsorption sites. At higher pHs (5–8), most of sulfate and carboxylate groups are deprotonated and the strong electrostatic interactions between negatively charged groups on the hydrogel nanocomposites and positively charged molecules of CV cause an enhancement of the adsorption capacity. The reason of the adsorption-loss for the highly basic solutions (pHs 9–13) is "charge screening effect" of excess Na^+ in the swelling media which shield the sulfate and carboxylate anions and prevent effective adsorption of CV molecules on the hydrogel nanocomposites.

Adsorption Isotherms

Different models like Langmuir and Freundlich have been developed for describing the behavior of adsorbent materials. The interactions between adsorbate and adsorbent to achievement of equilibrium adsorption can be studied using these adsorption isotherms. The adsorption isotherms describe the optimized adsorption system as well as the effectiveness of adsorbents. In fact, it is important to obtain an optimum isotherm model indicating the CV adsorption system onto the synthesized hydrogel nanocomposites. So, in these series of experiments, the practical data were fitted to the Langmuir and Freundlich models (Table 2). In the Langmuir adsorption model, adsorption of adsorbate takes place at specific homogeneous sites within the adsorbent and valid for monolayer adsorption onto adsorbents. But, the Freundlich model applies to adsorption on heterogeneous surfaces with interaction between adsorbed molecules[40].

The coefficients and non-linear R^2 values for both isotherm models are given in Table 2. The R^2 values for the Langmuir (0.988) and Freundlich (0.856) models depicts that the Langmuir isotherm has the best fit on

Table 2. Constants for adsorption of CV onto hydrogel nanocomposites according to the Langmuir and Freundlich isotherm models

	Langmuir			Freundlich		
	q_m	K_L	R^2	$1/n$	K_F	R^2
Hydrogel nanocomposite (0.03 wt % MCNT)	104	0.023	0.975	0.35	12.54	0.856
Hydrogel nanocomposite (0.07 wt % MCNT)	118	0.029	0.988	0.31	16.34	0.848

experimental data than the Freundlich model. Hence, it is possible to say that adsorption mechanism of CV on nanocomposite can be explained with a simple physical adsorption. But chelating effect of the functional groups onto the hydrogel nanocomposites are also thought to take part in the adsorption process. According to the Langmuir model, the maximum of CV adsorption capacity (118 mg · g^{-1}) onto hydrogel nanocomposites was obtained.

Table 3 shows some different materials used in the removal of CV and its sorption capacity values. According to these data, the adsorption capacity of the synthesized hydrogel nanocomposites in this study is comparative with that of other adsorbents. It shows that the hydrogel nanocomposite studied in this work has acceptable adsorption capacity.

Table 3. Comparison of sorption capacities by different adsorbent materials for CV dye

Adsorbent	Adsorption capacity [mg · g^{-1}]	References
Poly(AA-AM-MA)[a]	35	[27]
Raw kaolin	26	[29]
Bagasse fly ash	79	[41]
CarAlg/MMt[b]	89	[30]
Activated carbon	65	[42]
Activated carbon	175	[43]
Sewage sludge	263	[44]
Raw bentonite	130	[45]
Modified bentonite	457	[45]
Chitosan–BA[c]	18	[46]
PVBC beads[d]	160	[47]
Ball clay	169	[48]
Magnetic κ-Carb[e]	85	[49]
κC-poly(AA)/MCNT[f]	118	This work

[a] Poly(acrylic acid-acrylamide-methacrylate),
[b] Carageenan-Alginate/ Montmorillonite nanocomposite hydrogels,
[c] Chitosan-g-(4-hydroxybenzoic acid),
[d] Poly (vinyl benzyl chloride) beads,
[e] Magnetic kappa-carrageenan beads,
[f] kappa-carrageenan-poly(acrylic acid)/multi-walled carbon nanotube.

Reusability

One of the most important properties of adsorbents is its reusability after a particular process. For obtaining the reusability of the hydrogel nanocomposites, the adsorption-desorption cycle was repeated ten times with the same adsorbent (data not shown). It was observed that the adsorption capacity did not considerably change after ten cycles. Again, this result shows that the synthesized nanocomposites are good reusable CV adsorbent materials.

CONCLUSIONS

In the present work, a new hydrogel nanocomposite composed of carrageenan and multi-walled carbon nanotube was synthesized by in situ graft polymerization of acrylic acid monomer in the presence of methylene bisacrylamide as a cross-linker. The so obtained modified hydrogel was used for adsorption of crystal violet from aqueous solution. The adsorption capacity of nanocomposites was found to vary with MCNT concentration and agitation time as well as initial pH of solution.

The data also show that the CV adsorption onto the hydrogel nanocomposites obey the Langmuir isotherm model. Overall, the obtained results suggested that the hydrogel nanocomposites synthesized in this work could be used as an effective adsorbent for adsorption of cationic dyes from aqueous solutions.

LITERATURE CITED

1. Buchholz, F.L. & Graham, A.T. (1997). *Modern Superabsorbent Polymer Technology*, Wiley, New York.
2. Singh, B. & Pal, L. (2008). Development of sterculia gum based wound dressings for use in drug delivery. *Eur. Polym. J.* 44, 3222–3230. DOI: 10.1016/j.eurpolymj.2008.07.013.
3. Sorbara, L., Jones, L. & Williams, L.D. (2009). Contact lens induced papillary conjunctivitis with silicone hydrogel lenses. *Contac. Len. Anter. Eye* 32, 93–96. DOI: 10.1016/j.clae.2008.07.005.
4. Mao, L., Hu, Y., Piao, Y., Chen, X., Xian, W. & Piao, D. (2005). Structure and character of artificial muscle model constructed from fibrous hydrogel. *Curr. Appl. Phys.* 5, 426–428. DOI: 10.1016/j.cap.2004.11.003.
5. Lee, C.T., Kung, P.H. & Lee, Y.D. (2005). Preparation of poly (vinyl alcohol)chondroitin sulfate hydrogel as matrices in tissue engineering. *Carbohyd. Polym.* 61, 348–354. DOI: 10.1016/j.carbpol.2005.06.018.
6. Wu, J., Wei, W., Lian, Y.W., Su, Z.G. & Ma, G.H. (2007). A thermosensitive hydrogel based on quaternized chitosan and poly(ethylene glycol) for nasal drug delivery system. *Biomaterials* 28, 2220–2232. DOI: 10.1016/j.biomaterials.2006.12.024.
7. He, H., Cao, X. & Lee, L.J. (2004). Design of a novel hydrogel-based intelligent system for controlled drug release. *J. Control. Rel.* 95, 391–402. DOI: 10.1016/j.jconrel.2003.12.004.
8. Lin, Y., Chen, Q. & Luo, H. (2007). Preparation and characterization of N-(2-carboxybenzyl) chitosan as a potential pH-sensitive hydrogel for drug delivery. *Carbohydr. Res.* 342, 87–95. DOI: 10.1016/j.carres.2006.11.002.
9. Crini, G. (2005). Recent developments in polysaccharide-based materials used as adsorbents in wastewater treatment. *Prog. Polym. Sci.* 30, 38–70. DOI: 10.1016/j.progpolymsci.2004.11.002.
10. Wang, S.F., Shen, L., Zhang, W.D. & Tong, Y.J. (2005). Preparation and mechanical properties of chitosan/carbon nanotubes composites. *Biomacromolecules* 6, 3067–3072. DOI: 10.1021/bm050378v.
11. Coleman, J.N., Khan, U. & Gunko, K. (2006). Mechanical reinforcement of polymers using carbon nanotubes. *Adv. Mater.* 18, 689–706. DOI: 10.1002/adma.200501851.
12. Estrada, A.C., Daniel-da-Silva, A.L. & Trindade, T. (2013). Photothermally enhanced release by κ-carrageenan hydrogels reinforced with multi-walled carbon nanotubes. *RSC Adv.* 3, 10828–10836. DOI: 10.1039/C3RA40662H.
13. Ajayan, P.M., Stephan, O., Colliex, C. & Rauth, D.T. (1994). Aligned carbon nanotube arrays formed by cutting a polymer resin-nanotube composite. *Science* 265, 1212–1214. DOI: 10.1126/science.265.5176.1212.
14. Dai, L. & Mau, A.W.H. (2001). Controlled synthesis and modification of carbon nanotubes and C60: carbon nanostructures for advanced polymeric composite materials. *Adv. Mater.* 13, 899–913. DOI: 10.1002/1521-4095(200107)13:12/13.
15. Baughman, R.H., Zakhidov, A.A. & Heer, W.A. (2002). Carbon nanotubes-the route toward applications. *Science* 197, 787–792. DOI: org/10.1126/science.1060928.
16. Spitalsky, Z., Tasis, D., Papagelis, K. & Galiotis, C. (2010). Carbon nanotube-polymer composites: chemistry, processing, mechanical and electrical properties. *Prog. Polym. Sci.* 35, 357–401. DOI: 10.1016/j.progpolymsci.2009.09.003.
17. Iijima, S. (1991). Helical microtubules of graphitic carbon. *Nature* 354, 56–58. DOI: 10.1038/354056a0.
18. Allen, A., Cannon, A., Lee, J., King, W.P. & Graham, S. (2006). Flexible microdevices based on carbon nanotubes.

J. Micromech. Microeng. 16, 2722–2729. DOI: 10.1088/0960-1317/16/12/027.

19. Sippel-Oakley, J., Wang, H.T., Kang, B.S., Wu, Z., Ren, F., Rinzler, A.G. & Pearton, S.J. (2005). Carbon nanotube films for room temperature hydrogen sensing. *Nanotechnology* 16, 2218–2221. DOI: 10.1088/0957-4484/16/10/040.

20. Takenobu, T., Takahashi, T., Kanbara, T., Tsukagoshi, K., Aoyagi, Y. & Iwasa, Y. (2006). High-performance transparent flexible transistors using carbon nanotube films. *Appl. Phys. Lett.* 88, 033511. DOI: 10.1063/1.2166693.

21. Tang, X., Bansaruntip, S., Nakayama, N., Yenilmez, E., Chang, Y.L. & Wang, Q. (2006). Carbon nanotube DNA sensor and sensing mechanism. *Nano Lett.* 6, 1632–1636. DOI: 10.1021/nl060613v.

22. Chatterjee, S., Chatterjee, T. & Woo, S.H. (2010). A new type of chitosan hydrogel sorbent generated by anionic surfactant gelation. *Bioresour. Technol.* 101, 3853–3858. DOI: 10.1016/j.biortech.2009.12.089.

23. Li, Y.H., Wang, S., Wei, J., Zhang, X., Xu, C., Luan, Z., Wu, D. & Wei, B. (2002). Lead adsorption on carbon nanotubes. *Chem. Phys. Lett.* 357, 263–266. DOI: 10.1016/S0009--2614(02)00502-X.

24. Peng, X., Li, Y., Luan, Z., Di, Z., Wang, H., Tian, B. & Jia, Z. (2003). Adsorption of 1,2-dichlorobenzene from water to carbon nanotubes. *Chem. Phys. Lett.* 376, 154–158. DOI: 10.1016/S0009-2614(03)00960-6.

25. Chatterjee, S., Lee, D.S., Lee, M.W. & Woo, S.H. (2009). Enhanced adsorption of Congo red from aqueous solutions by chitosan hydrogel beads impregnated with cetyl trimethyl ammonium bromide. *Bioresour. Technol.* 100, 2803–2809. DOI: 10.1016/j.biortech.2008.12.035.

26. Pourjavadi, A., Hosseini, S.H., Seidi, F. & Soleyman, R. (2012). Magnetic removal of crystal violet from aqueous solutions using polysaccharide-based magnetic nanocomposite hydrogels. *Polym. Int.* 62, 1038–1044. DOI: 10.1002/pi.4389.

27. Li, S. (2010). Removal of crystal violet from aqueous solution by sorption into semi-interpenetrated networks hydrogels constituted of poly(acrylic acid-acrylamide-methacrylate) and amylase. *Bioresource Technol.* 101, 2197–2202. DOI: 10.1016/j.biortech.2009.11.044.

28. Singh, K.P., Gupta, S., Singh, A.K. & Sinha, S. (2011). Optimizing adsorption of crystal violet dye from water by magnetic nanocomposite using response surface modeling approach. *J. Hazard. Mater.* 186, 1462–1473. DOI: 10.1016/j.jhazmat.2010.12.032.

29. Nandi, B.K., Goswami, A., Das, A.K., Mondal, B. & Purkait, M.K. (2008). Kinetic and equilibrium studies on the adsorption of crystal violet dye using kaolin as an adsorbent. *Sep. Sci. Technol.* 43, 1382–1403. DOI: 10.1080/01496390701885331.

30. Mahdavinia, G.R., Aghaie, H., Sheykhloie, H., Vardini, M.T. & Etemadi, H. (2013). Synthesis of CarAlg/MMt nanocomposite hydrogels and adsorption of cationic crystal violet. *Carbohydr. Polym.* 98, 358–365. DOI: 10.1016/j.carbpol.2013.05.096.

31. Chatterjee, S., Chatterjee, T., Lim, S.R. & Woo, S.H. (2011). Effect of the addition mode of carbon nanotubes for the production of chitosan hydrogel core-shell beads on adsorption of Congo red from aqueous solution. *Biores. Tech.* 102, 4402–4409. DOI: 10.1016/j.biortech.2010.12.117.

32. Hosseinzadeh, H., Pourjavadi, A. & Zohuraan-Mehr, M.J. (2004). Modified carrageenan. 2. Hydrolyzed crosslinked κ-carrageenan-g-PAAm as a novel smart superabsorbent hydrogel with low salt sensitivity. *J. Biomater. Sci. Polymer Edn.* 15, 1499–1511. DOI: 10.1163/1568562042459715.

33. Sjostrom, E. (1981). *Wood Chemistry: Fundamental and Applications*, Academic Press, Chap. 9.

34. Park, S.J., Cho, M.S., Lim, S.T., Choi, H.J. & Jhon, M.S. (2003). Synthesis and dispersion characteristics of multi-walled carbon nanotube composites with poly(methyl methacrylate) prepared by in-situ bulk polymerization. *Macromol. Rapid Commun.* 24, 1070–1073. DOI: 10.1002/marc.200300089.

35. Blond, D., Barron, V., Ruether, M., Ryan, K.P., Nicolosi, V., Blau, W.J. & et al. (2006). Enhancement of modulus, strength, and toughness in poly(methyl methacrylate)-based composites by the incorporation of poly(methyl methacrylate)-functionalised nanotubes. *Adv. Funct. Mater.* 16, 1608–1614. DOI: 0.1002/adfm.200500855.

36. Yu, J.G., Zhao, X.H., Yang, H., Chen, X.H., Yang, Q., Yu, L.Y., Jiang, J.H. & Chen, X.Q. (2014). Aqueous adsorption and removal of organic contaminants by carbon nanotubes. *Sci. Total Environ.* 482–483, 241–251. DOI: 10.1016/j.scitotenv.2014.02.129.

37. Yu, J.G., Zhao, X.H., Yu, L.Y., Jiao, F.P., Jiang, J.H. & Chen, X.Q. (2014). Removal, recovery and enrichment of metals from aqueous solutions using carbon nanotubes. *J. Radioanal. Nucl. Ch.* 299, 1155–1163. DOI: 10.1007/s10967-013-2818-y.

38. Crini, G. & Badot, P.M. (2008). Application of chitosan, a natural aminopolysaccharide, for dye removal from aqueous solutions by adsorption processes using batch studies: a review of recent literature. *Prog. Polym. Sci.* 33, 399–447. DOI: 10.1016/j.progpolymsci.2007.11.001.

39. Nabid, M.R., Sedghi, R., Sharifi, R., Abdi-Oskooie, H. & Heravi, M.M. (2013). Removal of toxic nitrate ions from drinking water using conducting polymer/MWCNTs nanocomposites. *Iran. Polym. J.* 22, 85–92. DOI: 10.1007/s13726-012-0106-2.

40. Piccin, J.S., Gomes, C.S., Feris, L.A. & Gutterres, M. (2012). Kinetics and isotherms of leather dye adsorption by tannery solid waste. *Chem. Eng. J.* 183, 30–38. DOI: 10.1016/j.cej.2011.12.013.

41. Mall, I.D., Srivastava, V.C. & Agarwal, N.K. (2006). Removal of orange-G and methyl violet dyes by adsorption onto bagasse fly ash-kinetic study and equilibrium isotherm analyses. *Dyes Pigment.* 69, 210–223. DOI: 10.1016/j.dyepig.2005.03.013.

42. Mohanty, K., Naidu, J.T., Meikap, B.C. & Biswas, M.N. (2006). Removal of crystal violet from wastewater by activated carbons prepared from rice husk. *Ind. Eng. Chem. Res. 45*, 5165–5171. DOI: 10.1021/ie060257r.

43. Wang, S. & Zhu, Z.H. (2007). Effects of acidic treatment of activated carbons on dye adsorption. *Dyes Pig. 75*, 306–314. DOI: 10.1016/j.dyepig.2006.06.005.

44. Otero, M., Rozada, F., Calvo, L.F., García, A.I. & Morán, A. (2003). Elimination of organic water pollutants using adsorbents obtained from sewage sludge. *Dyes Pig. 57*, 55–65. DOI: 10.1101/gr.4039406.

45. Eren, E. (2009). Removal of basic dye by modified Unye bentonite, Turkey. *J. Hazard. Mater.* 162, 1355–1363. DOI: 10.1016/j.jhazmat.2008.06.016.

46. Chao, A., Shyu, S., Lin, Y. & Mi, F. (2004). Enzymatic grafting of carboxyl groups on to chitosan-to confer on chitosan the property of a cationic dye adsorbent. *Biores. Tech.* 91, 157–162. DOI: 10.1016/S0960-8524(03)00171-8.

47. Kaner, D., Sarac, A., Senkal, B.F. (2010). Removal of dyes from water using crosslinked aminomethane sulfonic acid based resin. *Environ. Geochem. Health* 32, 321–325. DOI: 10.1007/s10653-010-9304-z.

48. Monash, P., Niwas, R. & Pugazhenthi, G. (2011). Utilization of ball clay adsorbents for the removal of crystal violet dye from aqueous solution. *Clean Techn. Environ. Policy* 13, 141–151. DOI: 10.1007/s10098-010-0292-6.

49. Mahdavinia, G.R., Iravani, S., Zoroufi, S. & Hosseinzadeh, H. (2014). Magnetic and K$^+$-cross-linked kappa-carrageenan nanocomposite beads and adsorption of crystal violet. *Iran. Polym. J.* 23, 335–344. DOI: 10.1007/s13726-014-0229-8.